

PROCEEDINGS OF SPIE

SPIDigitalLibrary.org/conference-proceedings-of-spie

SNPP and NOAA-20 VIIRS on-orbit geolocation trending and improvements

Lin, Guoqing Gary, Wolfe, Robert, Dellomo, John, Tan, Bin, Zhang, Ping

Guoqing Gary Lin, Robert E. Wolfe, John J. Dellomo, Bin Tan, Ping Zhang, "SNPP and NOAA-20 VIIRS on-orbit geolocation trending and improvements," Proc. SPIE 11501, Earth Observing Systems XXV, 1150112 (16 September 2020); doi: 10.1117/12.2569148

SPIE.

Event: SPIE Optical Engineering + Applications, 2020, Online Only

SNPP and NOAA-20 VIIRS on-orbit geolocation trending and improvements

Guoqing (Gary) Lin^{*a,b}, Robert E. Wolfe^b, John J. Dellomo^{c,b}, Bin Tan^{a,b}, Ping Zhang^{a,b}

^aScience Systems and Applications, Inc., 10210 Greenbelt Road, Lanham, MD 20706, USA;

^bNASA Goddard Space Flight Center, 8800 Greenbelt Rd, Greenbelt, MD 20771, USA;

^cGlobal Science & Technology, Inc., 7855 Walker Drive, Greenbelt, MD 20770, USA

ABSTRACT

Two Visible Infrared Imaging Radiometer Suite (VIIRS) sensors have been in operations for more than 8.5 and 2.5 years since they were launched in October 2011 on SNPP satellite and in November 2017 on NOAA-20 satellite, respectively. These are two satellites in the Joint Polar Satellite System (JPSS) constellation, of which Suomi National Polar-orbiting Partnership (SNPP) is a risk reduction satellite and NOAA-20 is the first of four JPSS satellites (JPSS-1 became NOAA-20 after launch). Accurate geolocation is a critical element in data calibration for accurate retrieval of global biogeophysical parameters. In this paper, we describe the latest trends in the continuously improved geolocation accuracy in VIIRS Collection-1 (C1) and C2 re-processing. We implemented a VIIRS instrument geometric model update (VIGMU) for both sensors that correct for geolocation error oscillations in the scan direction. We borrowed code from Moderate Resolution Imaging Spectroradiometer (MODIS) geolocation software to correct for time-dependent pointing variations, that are particularly acute in NOAA-20 VIIRS, and some pointing anomalies in SNPP VIIRS. We developed a Kalman Filter using gyro data to correct for attitude errors due to the degradation of the star trackers performance from the SNPP satellite. We also present an improved ground control point matching (CPM) tool, in which the ground control point (GCP) chips library is refreshed using recently launched Landsat-8 images.

Keywords: SNPP, NOAA-20, VIIRS, geolocation, pointing, error analysis, Kalman filter, trending

1. INTRODUCTION

The NASA/NOAA Visible Infrared Imaging Radiometer Suite (VIIRS) instrument onboard the Suomi National Polar-orbiting Partnership (SNPP) satellite has been operating^[1,2,3,4] since its launch on 28 October 2011. A second VIIRS instrument onboard the first Joint Polar Satellite System (JPSS-1, J01 or J1) spacecraft was launched on 18 November 2017, that became NOAA-20 (or N20)^[5,6]. SNPP and N20 operate one-half orbit apart in a constellation in the same orbital plane at an average altitude of 838.8 km above the Earth surface^[6]. The nominal design of these VIIRS instruments are the same, with some minor differences in the as-built and the as-operated radiometric and geometric parameters^[6,7,8]. VIIRS has 5 imagery bands (I-bands), 16 moderate radiometric bands (M-bands) and a panchromatic Day-Night band (DNB), covering spectral range from 0.4 μm to 12.4 μm ^[3]. The nominal resolution at nadir is 375 m for I-bands and 750 m for M-bands and DNB. Pixel size grows off-nadir to about twice as large to the edges of scan at $\sim\pm 56^\circ$ in the track direction for I-band and M-bands, while in the scan direction, a scheme in three sample aggregation zones limits the pixel growth to 2 times to the edges of scan^[1,2,3,6]. We use band I1 (red visible) as the primary band for geolocation error detection and correction, which is the focus of this paper.

This paper is organized as follows. Section 2 summarizes overall geolocation accuracy in VIIRS Collection 1 (C1) and C2 both forward processed and re-processed by NASA VIIRS Land Science Investigator-led Processing System (SIPS). Sections 3 details the time series of geolocation accuracies in SNPP VIIRS C1, and preparation for C2 re-processing with improvements including VIIRS instrument geometric model update (VIGMU), time-dependent correction for pointing variation, correction for pointing errors stemmed from on-orbit operations procedures, and improved attitude using ground-based Kalman filter. Sections 4 describes geolocation accuracies in C1 and C2, and the improvements in C2 with VIGMU and time-dependent correction for pointing variation, and preparation for upcoming C2.1 re-processing and incorporation of ground control point (GCP) refresh in control point matching (CPM) program. Section 5 gives concluding remarks.

*Gary.Lin@nasa.gov; glin@ssaihq.com; phone 301-614-5451; fax 301-614-5269; www.ssai.org

2. VIIRS RE-PROCESSING COLLECTIONS AND GEOLOCATION RESULTS SUMMARY

The Suomi National Polar-orbiting Partnership (SNPP) satellite was formerly known as the National Polar-orbiting Operational Environmental Satellite System (NPOESS) Preparatory Project (NPP) satellite. It was designed to serve as a bridge between NASA Earth Observing System (EOS) and the Joint Polar Satellite System (JPSS)^[9]. It also serves as a risk-reduction program. NPP was launched on 28 October 2011, and was renamed as Suomi National Polar-orbiting Partnership (SNPP) on 24 January 2012^[10]. The VIIRS land data products generated by the NASA Land Product Evaluation and Analysis Tool Element (PEATE) were assessed by the NASA Land Science Team^[11]. Other PEATEs generated other SNPP data products for assessments. These NASA PEATEs have evolved to the Science Investigator-led Processing Systems (SIPs). Data format for VIIRS Level-1 products in the Land SIPs is in a hybrid NetCDF4-HDF5 format^[12]. Collection-1 (C1) of SNPP VIIRS Level-1 data re-processing started on 11 October 2017, as illustrated in Figure 1. Data for all bands in VIIRS became available on 19 January 2012 when the cryo-radiator door was open^[1,2], which is the start date for all data Collections for SNPP VIIRS. For NOAA-20 VIIRS, data for all bands became available after the cryo-radiator door opened on 5 January 2018. After initial on-orbit geolocation calibration and validation activities^[6], C1 started 14 March 2012, as illustrated in Figure 1 in the lower part. That C1 forward-processing was terminated in January 2020 after C2 re-processing started on 12 July 2019. SNPP C2 and NOAA-20 C2.1 have been under preparation and will be available soon.

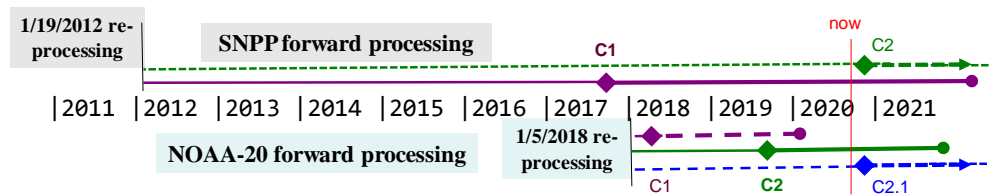


Fig. 1. Illustration of the VIIRS re-processing collections. The upper part is for SNPP VIIRS re-processing and forward-processing, while the lower part is for NOAA-20 VIIRS.

In re-processing, careful analysis has been applied to correct for geolocation biases in long-term trends based on the geolocation errors detected in the previous collection. The geolocation error detection program was inherited from EOS Moderate Resolution Imaging Spectroradiometer (MODIS) geolocation control point matching (CPM) program^[1,2,13] and was later improved^[6]. The geolocation accuracy presented in this paper is from the improved version of the CPM. As we will see later, the ground control point (GCP) library used in the CPM is being refreshed, further improving the CPM.

The overall geolocation accuracy assessments for the completed C1 and C2 are listed in Table 1. Both collections have good geolocation accuracy with means close to zero in C2 and the root-mean-square errors (RMSEs) less than 75 m (20% of I-band resolution). In general, the biases in mean errors in the track and scan directions are gradually reduced from each reprocessing. That is also true for the RMSEs. The improvements seem small for the whole collection or the mission-to-date. However, they result from corrections for larger biases that occurred for short time periods, as we will see in details in Sections 3 & 4. Note that in this paper the measured geolocation errors are all adjusted for scan angle and are expressed in nadir equivalent units.

Table 1. Each collection's overall VIIRS geolocation accuracy in nadir equivalent units.

Residuals	SNPP C1	NOAA-20 C1	NOAA-20 C2
Track mean	-14 m	0 m	-1m
Scan mean	5 m	-14 m	0 m
Track RMSE	59 m	58 m	55 m
Scan RMSE	52 m	55 m	49 m
Data-days (years)	3116 (8.5y)	758 (2.1y)	925 (2.5y)
Missing days	1	6	3
Daily matches	201	186	191

3. SNPP VIIRS GEOLOCATION ACCURACY IN C1

SNPP VIIRS geolocation went through early on-orbit calibration and validation^[1], and long term monitoring and correction in the early mission^[2]. A pointing error was detected due to star trackers realignment on 23 April 2013, 15:20 UTC. That error was corrected for in August 2013. Thus, two look-up tables (LUTs) were used for re-processing in C1, one before the star trackers realignment and another after. The time series of SNPP VIIRS C1 geolocation errors is shown in Figure 2.

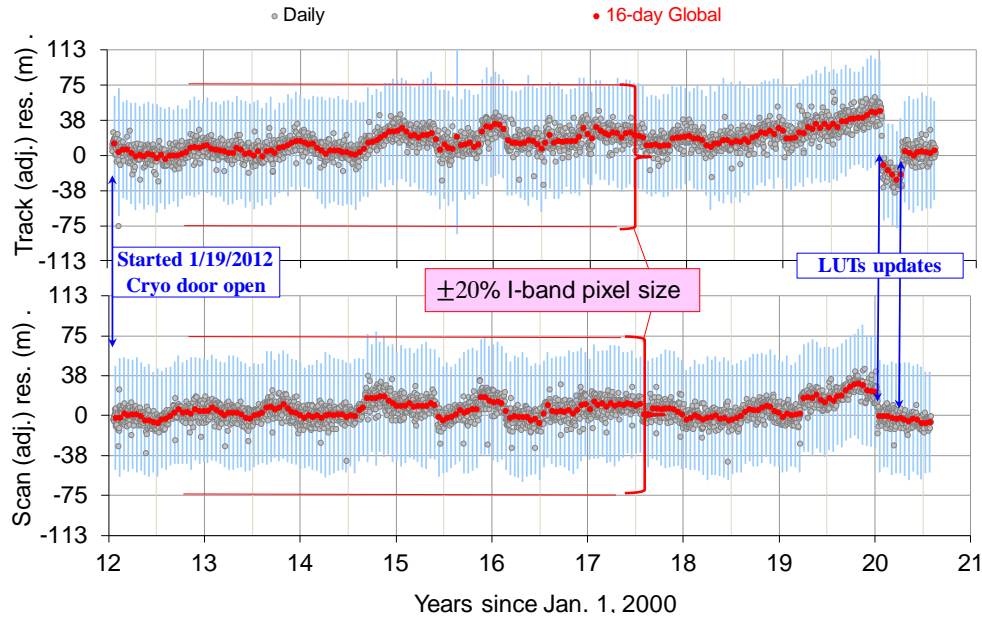


Fig. 2. Time series of SNPP VIIRS C1 geolocation errors. The error bars are 16-day statistics.

As we can see from Figure 2, there were other pointing variations during the SNPP mission. On 22 March 2019, there was an on-orbit operation that reset the star tracker-2. That somehow caused a small shift in pointing and drift afterward, especially in the pitch direction. We improved geolocation accuracy by updating instrument-to-spacecraft rotation angle in the LUT on 10 January 2020 and again on 26 March 2020.

Figure 3 shows the time-dependent instrument-to-spacecraft mounting interface (“inst2sc IF” in the y-axis of the plot) rotation angle corrections for C2 re-processing. We simplify all possible causes of pointing variations to this interface. The code was borrowed from MODIS geolocation processing software^[13, 14]. We tested to confirm the changes, including star trackers realignment on 23 April 2013 and scan control electronics side change on 22 November 2012, 16:32 UTC.

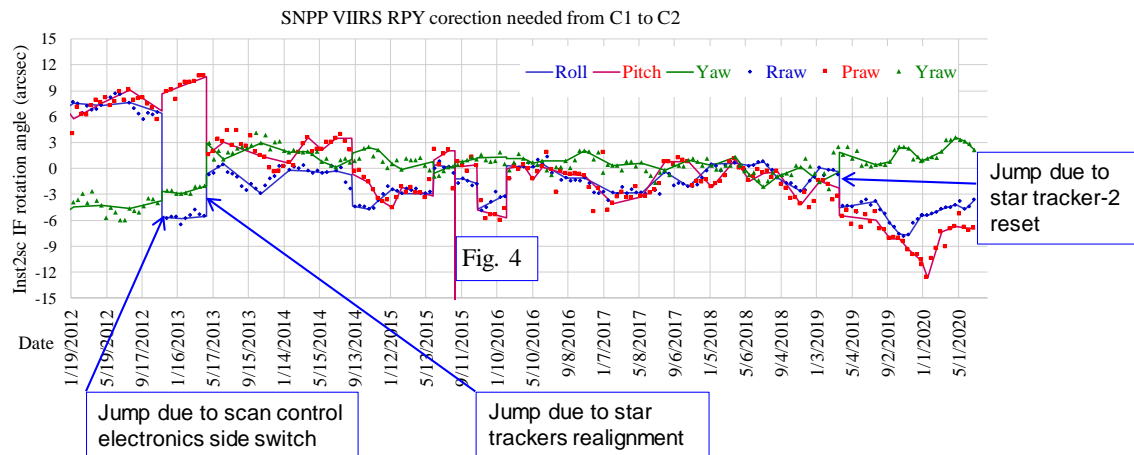


Fig. 3. Time series of instrument-to-spacecraft mounting angle corrections for SNPP VIIRS C2 geolocation.

In the process of searching for ways to improve the geolocation accuracy, we found a chunk of data having large geolocation errors, which was traced to spacecraft control computer (SCC) clock time error when a normal procedure for clock slope correction was performed. The time error was +1 second relative to the global positioning satellite (GPS) time, lasting from 14:24:40 to 21:16:30 UTC on 19 August 2015. This 1-second time error caused orbit propagator to pick up the spacecraft position 1 second ahead of the time from the spacecraft attitude determination and control system (ADCS). The ADCS had an attitude with pitch of -213 arc-seconds at first but then controlled the attitude toward 0 degrees, causing a knowledge error of 213 arc-seconds, which is the average amount of pitch in one orbit period of 6090 seconds. We artificially set an additional pitch of -213 arc-seconds in the instrument-to-spacecraft rotation angle in the LUT. The test results are shown in Figure 4. We have “saved” ~7 hours of data.

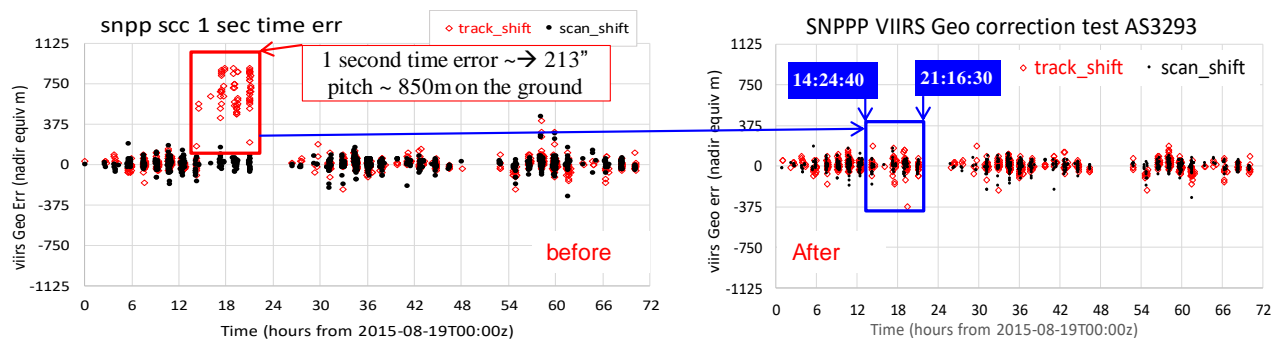


Fig. 4. Geolocation errors before and after correction for a 1-second time error in an equivalent of 213 arc-seconds in pitch.

The scan profiles of geolocation errors are shown in Figure 5. The measured errors are stratified every 1° in the scan angle for the mission-to-date. In the track direction, geolocation is biased in the positive direction by 10 to 20 meters. In the scan direction, the geolocation errors have a pattern, fluctuating between -20 and +20 meters. The problem mainly stems from VIIRS Half-Angle Mirror (HAM) motion non-linearity. The VIIRS rotating telescope assembly (RTA) motion non-linearity is small and not shown here. VIIRS geolocation processing software was supposedly to take care of the motion non-linearity as reflected in encoders (Figure 6). However, it was found that the image flip by the RTA was not incorporated in the algorithm. When we changed the RTA magnification parameter from the existing “+4” to new “-4”, the problem is resolved, see Section 4. We call this VIIRS instrument geometric model update (VIGMU).

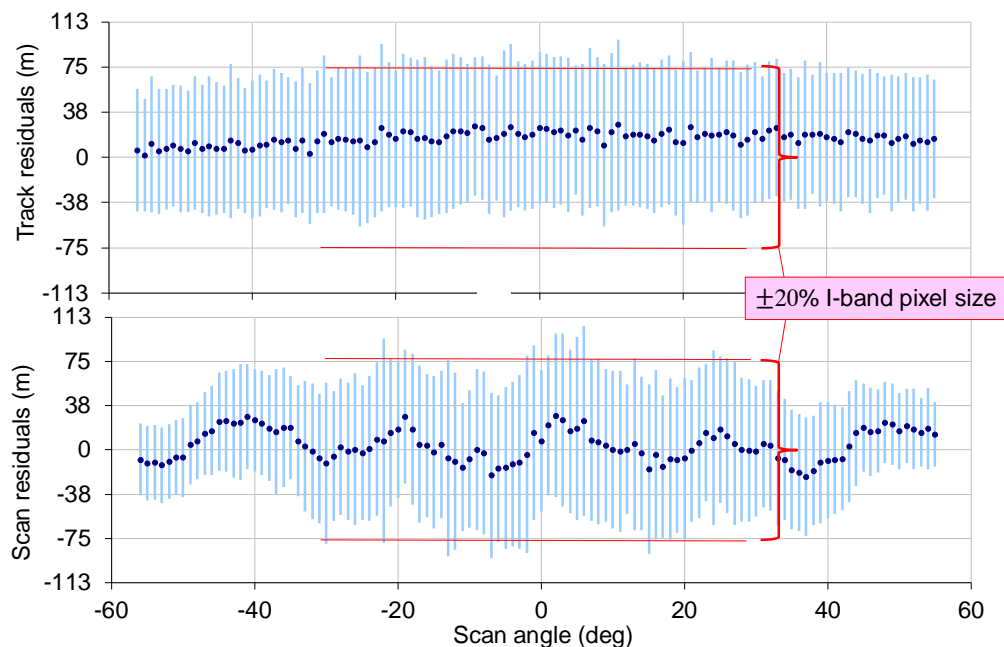


Fig. 5. SNPP VIIRS scan angle dependence of the geolocation errors (nadir equivalent). The means and error bars are 1° apart.

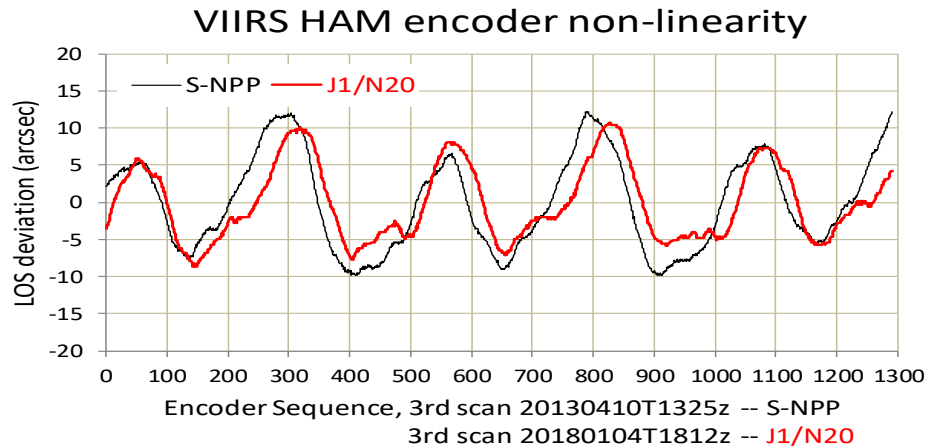


Fig. 6. SNPP and NOAA-20 VIIRS Half-Angle Mirror (HAM) encoder non-linearity.

We are also improving the SNPP attitude by ground-based Kalman Filter, along with the above mentioned time-dependent pointing error correction and VIGMU. Note, VIGMU causes some pointing change and the time series of instrument-to-spacecraft mounting angle corrections as shown in Figure 3 that are also taken into account.

After the first few years of the mission, we started seeing large SNPP attitude excursions on a regular basis. The specifications for the attitude performance are 1) control error within 108 arc-seconds in any axis in any one nominal operation orbit 99.73% of the time (3σ), and 2) knowledge error within 21 arc-seconds in any axis in any one nominal operation orbit 99.73% of the time (3σ). Figure 7 shows such a case. The attitude reported from the spacecraft shows the attitude control error (upper right plot). The attitude behaved oddly, besides have large jumps of about 300 arc-seconds the patterns are unrealistic. We used a ground-based Kalman filter^[15, 16] to estimate actual attitude using gyro data that were downlinked to the ground. Assuming that the Kalman filter processed attitude data are true, then the differences between the attitude data from Kalman Filter and those from the spacecraft are the knowledge errors. We did a study^[17] into this case by using the technique of land/water masking and by shifting the images in each scan to match the coastline segments in the western Australia from the data 16 days earlier, see sub-figures on the left-side of Figure 7. The amount the image shifts is compatible with the knowledge error shown in the upper-right plot.

We can easily detect control error specification outages. That detection gives us a trend of SNPP attitude determination and control system (ADCS) performance in the history of the mission-to-date (Figure 8, where y-axis is the root sum squared (RSS) of attitude errors in all three directions when one or more of them is out-of-specification.). As we can see, the ADCS degraded over time before the 5th anniversary. An action was taken on 21 and 22 September 2016 to lower the Thermal Electric Cooler (TEC) setpoint for the two Star Trackers' CCD arrays from 0°C to -10°C. That action improved the performance.

It is difficult to know when the knowledge error is out of specification. However, we can associate the knowledge error with the control error, as shown in the case in Figure 7. Given some margin, when the control errors exceed 36 arc-seconds (15 more than the specified 21 arc-seconds) 99.73% of the time (that is 17 or more second-points in a complete orbit of ~6090 seconds), we say the knowledge error is out-of-specification. The results of such detection are shown in Figure 8. Similar to control error specification outages, the knowledge error specification outages increased with time before the star trackers cooling. In the last 4 years, the ADCS has degraded again, but not as serious as that during the first 5-year time period.

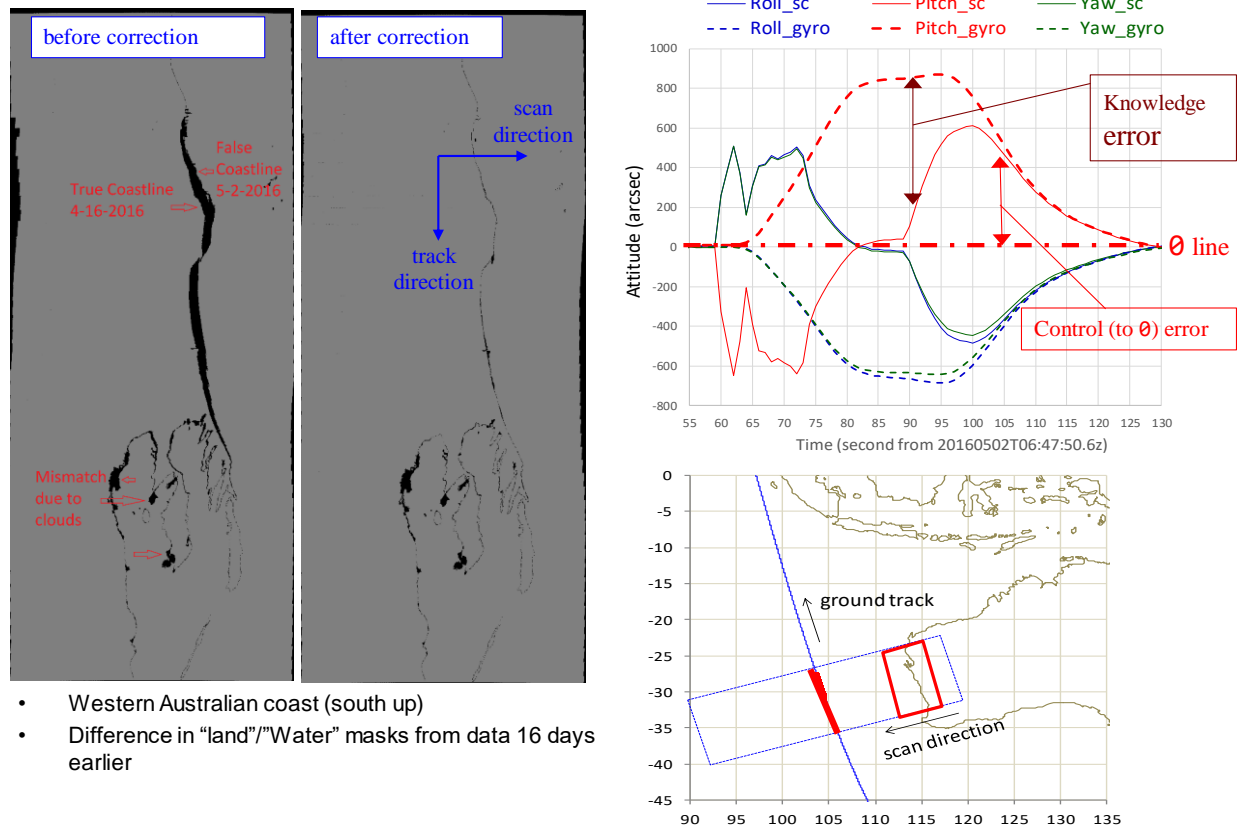


Figure 7. A case of SNPP attitude performance non-compliance. The lower right plot shows the location of the case. The upper right plot shows the attitude control and knowledge errors. The left two figures show attitude correction using the coastline matching.

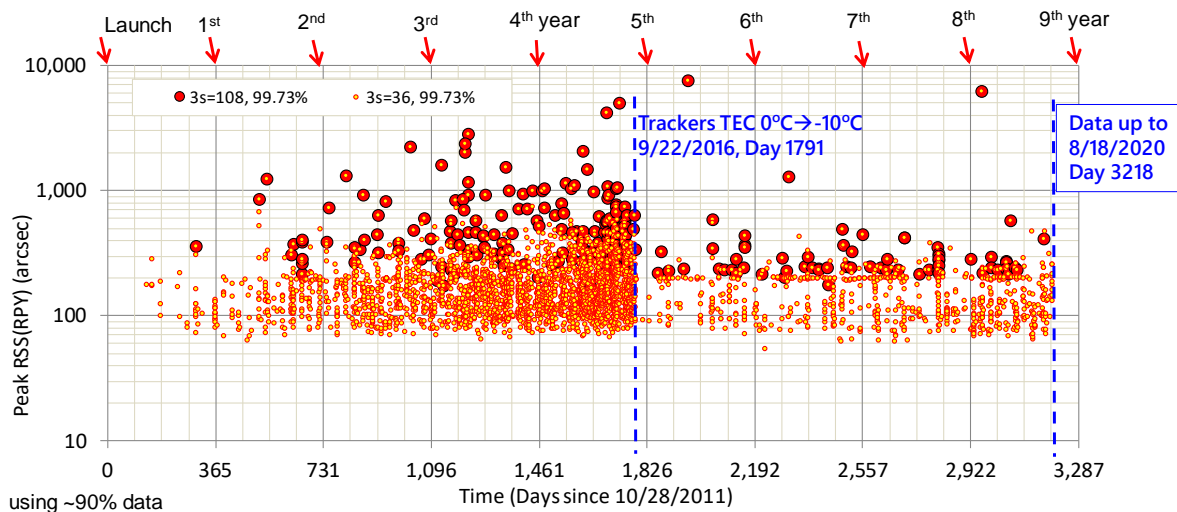


Figure 8. Trends of SNPP attitude performance. Large circles indicate control specification (108 arcsec, 3 σ) outage per orbit. Small dots hint knowledge specification (36 arcsec, 3 σ) outage. Star tracker cooling improved SNPP attitude performance.

In our SNPP C2 re-processing, we are employing the ground-based Kalman filter to improve the attitude performance, as shown as an example in the upper right plot in Figure 7.

4. NOAA-20 VIIRS GEOLOCATION ACCURACY IN C1 AND C2

NOAA-20 VIIRS geolocation went through early on-orbit calibration and validation^[6]. Collection-1 (C1) processing started 14 March 2012, with the visible and near-infrared (VisNIR) bands of I1, I2 and M1 to M7 data re-processed right after the nadir opened on 13 December 2017, and all bands data re-processed after the cryo-radiator door open on 5 January 2018. C1 data processing stopped on 16 January 2020 after C2 re-processing started on 12 July 2019 and its near-real-time forward-processed data became available to users. Figure 9 shows the time series of N20 VIIRS geolocation accuracy in C1 and C2. Note that in C1, C2 code and LUTs were applied on 30 May 2019 in forward processing, which resulted in identical geolocation accuracy between C1 and C2 after that date.

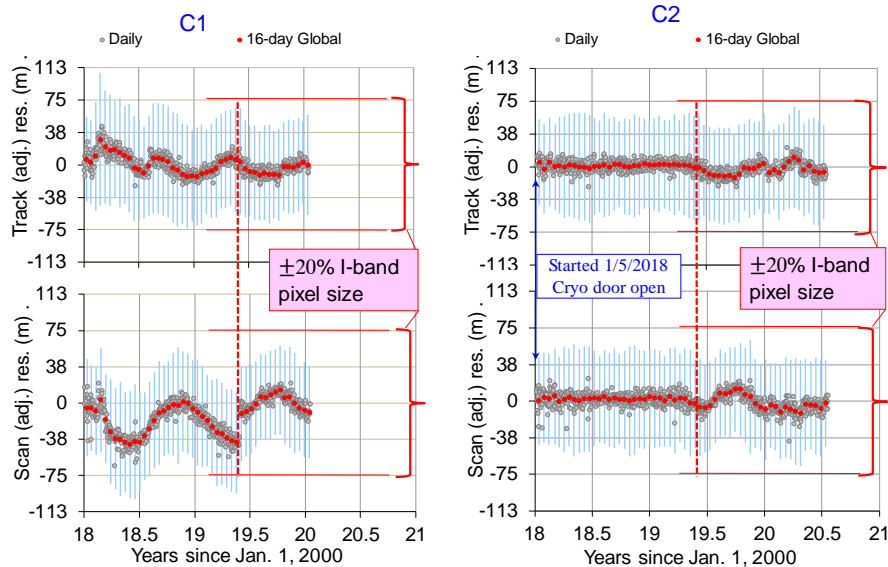


Fig. 9. Time series of N20 VIIRS geolocation accuracy. Left panels, C1 results; right panels, C2 results.

C2 code and LUTs implemented VIIRS instrument geometric model update (VIGMU) and correction for temporal pointing variation. The VIGMU takes scan motion non-linearity (Figure 6) into account by “restoring” image flipping in the RTA from using magnification $M = 4$ to $M = -4$ in the look-up table and some associate code (see details above in Section 3). After VIGMU, the pointing variation in the scan direction such as shown in Figure 5 for SNPP VIIRS is corrected for in N20 VIIRS as shown in Figure 10.

The temporal pointing variation in N20 VIIRS was first detected by geolocation errors measured by the control point matching (CPM) program in C1. As shown in Figure 9, the daily means of geolocation errors vary with time in both scan and track directions. The trends in 16-day means are clearer. These can be used to calculate pointing variations in pitch and roll rotation angles at the instrument-to-spacecraft interface that correspond to 16-day mean errors in the track and scan directions, respectively. The pointing variation in the yaw direction is reflected in the 16-day standard deviations (error bars) in Figure 9. It can be calculated as a function of slope in scan angle dependence of the geolocation errors (locally measured, not nadir equivalent) similar to the plot in the upper panel in Figure 10. These calculations are implemented in a program using statistical values of geolocation error measurements in each 16-day period stratified in scan angle bins in 1° increment^[2,13]. The results of pointing variations using C1 data are shown in solid curves in Figure 11 before mid-2019.

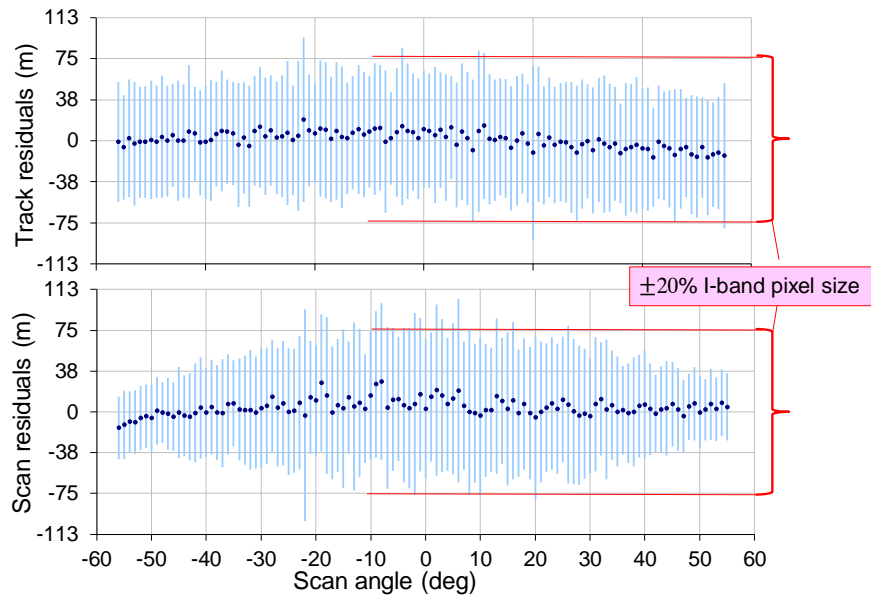


Fig. 10. .N20 VIIRS scan angle dependence of the geolocation errors (nadir equivalent).

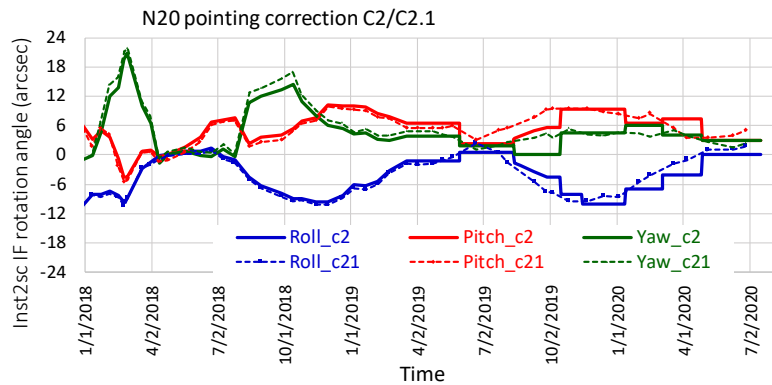


Fig. 11. Time series of instrument-to-spacecraft mounting angle corrections for SNPP VIIRS C2 geolocation.

Figure 11 also shows pointing corrections for the upcoming C2.1 based on geolocation error measurements in C2. Note that pointing corrections for C2 processing have distinguished features in two periods, which are roughly delineated by the time the C2 code the LUTs are switched on in C1 forward-processing in mid-2019. The period before mid-2019 used fully processed C1 data to calculate the time series of pointing variations and used them in the LUTs for C2 re-processing. Also note that on 25 April 2018, pointing angles were adjusted to 0 as we tested the VIGMU between 7 April 2018 and 8 May 2018, and adjusted the constant instrument-to-spacecraft interface matrix in the LUTs. In the period after mid-2019, both C1 and C2 were in forward processing mode in that we predicted possible pointing variations in a future duration such as 30 or 60 days. Then we monitored pointing variation as data became available. When that pointing variation became too large, say, more than 3 arc-seconds, we update the LUTs for use for another 30 or 60 days. That is the reason we see stair-step shape of the pointing variations in the second period in Figure 11. These inaccuracies in the pointing predictions are corrected for in C2.1.

All of the above geolocation errors are expressed in nadir equivalent unit, that is, any error measured at any local position corresponding to the scan angle at that position is projected to nadir position. That projection “reduces” measured geolocation error at the edges of a scan at a rate of about 2 times in the track direction and about 6 times in the scan direction, assuming that the geolocation errors are purely caused by attitude knowledge errors. Figure 12 shows such local geolocation errors in the scan direction, which is a “restoration” of lower panel in Figure 10.

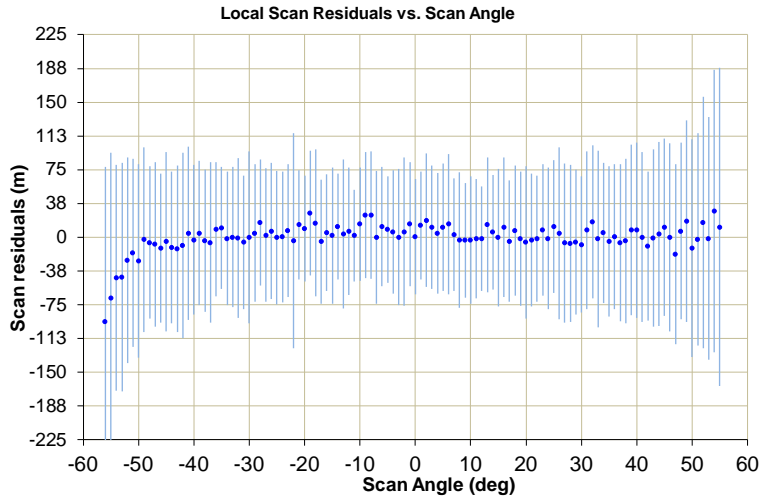


Fig. 12. Statistics of N20 VIIRS “local” geolocation errors versus scan angles.

As we can see from Figure 12, geolocation errors increase in magnitude as scan angle approaches the start of scan at -56° . This is speculated to be caused by atmospheric refraction^[18,19,20]. However, the trend on the right side of the figure is not clear. The uncertainties are also high. We hope to be more certain after applying the ground control point (GCP) refresh.

The existing GCP library has over 1200 image chips (Figure 13a) acquired around 2000 from Landsat-5 and Landsat-7 scenes. It has been used for MODIS geolocation error detection with the development of control point matching (CPM) program^[13,21]. The CPM program was adapted for us in SNPP VIIRS geolocation error detection^[2] and improved^[6] for use starting from C1 in SNPP VIIRS and N20 VIIRS.

We have observed that the number of successful control point matches slowly declines over time, probably due to changes in land use or geographical morphology. The annual rate of change is small, about 2 daily matches less in the current year than those in the previous year on average. Table 1 shows that SNPP VIIRS has more daily matches than N20 VIIRS because SNPP mission started earlier. Daily control point matches for MODIS sensors on Terra and Aqua have similar trends, which are not shown here but that actually triggered us to start the GCP refresh^[14]. The new GCP image chips were recently acquired from Landsat-8 scenes, and the library has about 2500 image chips (Figure 13b). A 16-day test for N20 VIIRS has shown that there are about 5 times more daily matches by using the new library than matches using the existing library. We plan to use the new library in SNPP VIIRS C2 and N20 VIIRS C2.1.

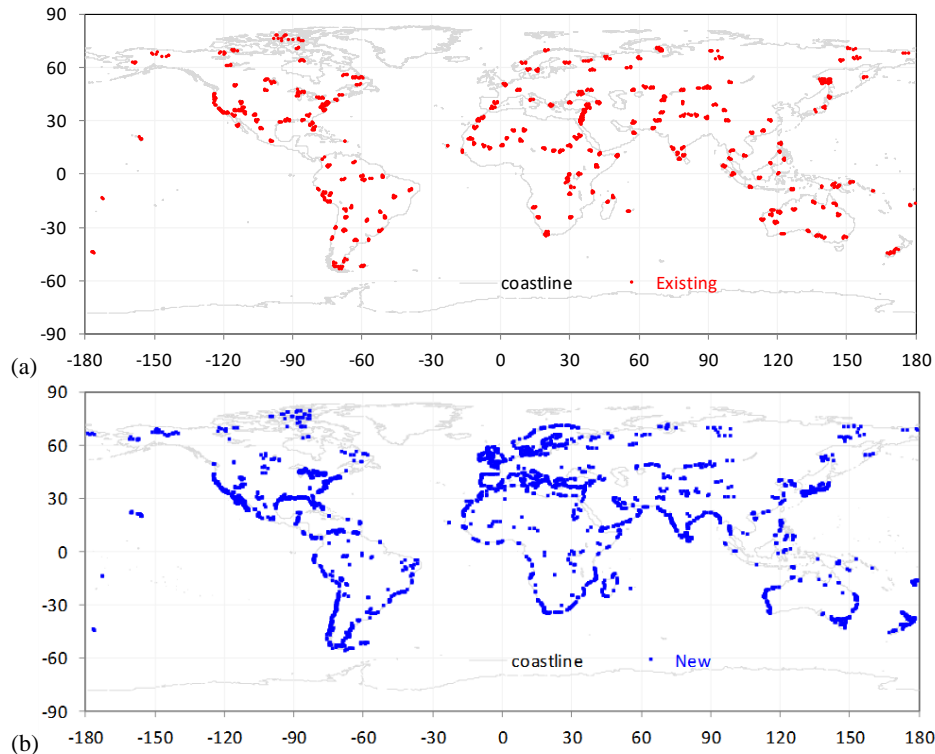


Fig. 13. Global distribution of ground control point (GCP) image chips. (a) Existing GCP chips used in MODIS and VIIRS control point matching (CPM) programs; (b) New GCP chips.

5. CONCLUDING REMARKS AND PATHS FORWARD

The SNPP and NOAA-20 VIIRS sensors have been successfully operated on orbit for more than 8.5 years and 2.5 years, respectively. Geolocation accuracy for both sensor is very good. Daily mean geolocation biases are within ± 0.1 I-band pixels, and the standard deviations are within about 20% pixels.

For SNPP VIIRS, Collection-2 (C2) re-processing by NASA Land Science Investigator-led Processing System (SIPS) is underway, implementing time-based pointing error corrections (including spacecraft clock error), VIIRS instrument geometric model update (VIGMU), and Kalman filter for improving attitude performance. C2 processing for N20 VIIRS has already started one year ago, which implemented time-based pointing error corrections and VIGMU, and is on the way toward C2.1 for further corrections in the inaccuracies in pointing predictions in the forward-processing part of C2.

There are always prediction inaccuracies in forward-processing that will be corrected for in future re-processing Collections. In the meantime, we are seeking other improvements, including ground control point (GCP) image chip refresh in control point matching (CPM) program, digital elevation model (DEM) upgrade from current 1 km version to more recent 500 m or 250 m database (not discussed in the text), and possible correction for atmospheric refraction.

ACKNOWLEDGEMENTS

The authors acknowledge the sponsorship of this work by NASA JPSS Project Science Office and NOAA Center for Satellite Applications and Research (STAR), and the cooperation and assistance from many colleagues from Raytheon Company, the NASA VIIRS Land SIPS, the VIIRS Characterization Support Team (VCST) Radiometric Group, and Fred Patt of Science Applications International Corporation (SAIC) on-site on NASA Goddard Space Flight Center.

REFERENCES

- [1] Wolfe, R.E., G. Lin, M. Nishihama, K.P. Tewari, E. Montano (2012), "NPP VIIRS Early On-Orbit Geometric Performance", Earth Observing Systems XVII, edited by J. J. Butler, X. Xiong, X. Gu, *Proc. of SPIE* Vol. 8510, 851013, doi: 10.1117/12.929925.
- [2] Wolfe, R.E., G. Lin, M. Nishihama, K. P. Tewari, J. C. Tilton, A. R. Isaacman (2013), "Suomi NPP VIIRS prelaunch and on-orbit geometric calibration and characterization", *Journal of Geophysical Research – Atmospheres*, VOL. 118, 11,508–11,521, doi: 10.1002/jgrd.50873.
- [3] Cao, C., F. DeLuccia, X. Xiong, R. Wolfe, F. Weng (2014), "Early On-orbit Performance of the Visible Infrared Imaging Radiometer Suite (VIIRS) onboard the Suomi National Polar-orbiting Partnership (S-NPP) Satellite," *IEEE Trans. Geosci. Remote Sens.*, vol. 52, no. 2, pp. 1142–1156, DOI:10.1109/TGRS.2013.2247768.
- [4] Tilton, J. C, G. Lin, and B. Tan (2016), "Measurement of the Band-to-Band Registration of the SNPP VIIRS Imaging System From On-Orbit Data", *Journal of Selected Topics in Applied Earth Observations and Remote Sensing*, Vol. 10, No.3, March 2017, pp. 1056-1067; DOI: 10.1109/JSTARS.2016.2601561.
- [5] Tilton, J. C., R.E. Wolfe, G. Lin, and J.J. Dellomo (2019), "On-Orbit Measurement of the Effective Focal Length and Band-to-Band Registration of Satellite-Borne Whiskbroom Imaging Sensors." *J. of Selected Topics in Applied Earth Observations and Remote Sensing*, VOL. 12, NO. 11, pp4622-4633, doi: 10.1109/JSTARS.2019.2949677.
- [6] Lin, G., R. E. Wolfe, J. C. Tilton, P. Zhang, J. J. Dellomo, B. Tan (2018), "JPSS-1/NOAA-20 VIIRS early on-orbit geometric performance", *Proc. SPIE* 10764, Earth Observing Systems XXIII, 107641H, doi: 10.1117/12.2320767.
- [7] Lin, G., R. E. Wolfe, M. Nishihama (2012), "NPP VIIRS Geometric Performance Status", Earth Observing Systems XVI, edited by James J. Butler, Xiaoxiong Xiong, Xingfa Gu, *Proc. of SPIE* Vol. 8153, 81531V, doi: 10.1117/12.894652.
- [8] Lin, G., and R. E. Wolfe (2016), "JPSS-1 VIIRS at-launch geometric performance." Earth Observing Systems XXI, edited by J. J. Butler, X. Xiong, X. Gu, *Proc. of SPIE* Vol. 9972, 99721L, doi: 10.1117/12.2238804.
- [9] https://www.nasa.gov/mission_pages/NPP/mission_overview/index.html (accessed 8/28/2020)
- [10] https://en.wikipedia.org/wiki/Suomi_NPP (accessed 8/28/2020).
- [11] Justice, C., M. O. Román, I. Csizsar, E. F. Vermote, R. E. Wolfe, S. J. Hook, M. Friedl, Z. Wang, C. B. Schaaf, T. Miura, M. Tschudi, G. Riggs, D. K. Hall, A. I. Lyapustin, S. Devadiga, C. Davidson, E. J. Masuoka (2013), "Land and cryosphere products from Suomi NPP VIIRS: Overview and status." *J. Geophys. Res. Atmos.*, 118 (17): 9753-9765, doi: 10.1002/jgrd.50771.
- [12] https://ladsweb.modaps.eosdis.nasa.gov/missions-and-measurements/viirs/NASA_VIIRS_L1B_UG_May_2018.pdf (accessed 8/28/2020)
- [13] Wolfe, R.E. and M. Nishihama (2011), "Accurate MODIS global geolocation through automated ground control image matching," in *Image Registration for Remote Sensing*, J. Le Moigne, N. S. Netanyahu and R. D. Eastman (eds.), Cambridge Univ. Press, New York, pp. 437-455, doi: 10.1017/cbo9780511777684.022.
- [14] Lin, G., R.E. Wolfe, P. Zhang, J. C. Tilton, J. J. Dellomo, B. Tan (2019), "Thirty-six combined years of MODIS geolocation trending," *Proc. SPIE* 11127, Earth Observing Systems XXIV, 1112715, doi: 10.1117/12.2529447.
- [15] Patt, F. S., "Analysis of the SNPP Gyro Data", December 2016, unpublished.
- [16] Patt, F. S., "A Kalman Smoother Algorithm for Refinement of the SNPP Attitude", June 2017, unpublished.
- [17] Tilton, J. C. and G. Lin, (2016) "SNPP Attitude Performance and Error Analysis Using VIIRS Geolocation," unpublished.
- [18] Noerdlinger, Peter D. (1999), "Atmospheric refraction effects in Earth remote sensing," *ISPRS J. of Photogrammetry & Remote Sensing*, 54, 360–373
- [19] Yan, M., C. Wang, J. Ma, Z. Wang, and B. Yu (2016), "Correction of atmospheric refraction geolocation error for high resolution optical satellite pushbroom images," *Photogrammetric Engineering & Remote Sensing* Vol. 82, No. 6, pp. 427–435, doi: 10.14358/PERS.82.6.427.
- [20] Gao, Bo-Cai, personal communication.
- [21] Wolfe, R. E., M. Nishihama, A.J Fleig, J.A Kuyper, D.P Roy, J.C Storey, F.S Patt (2002), "Achieving sub-pixel geolocation accuracy in support of MODIS land science." *Remote Sensing of Environment*, 83, pp. 31-49.